

Anisotropic matter and nonlinear electromagnetics black holes

Yun Soo Myung¹ and Wonwoo Lee²

Center for Quantum Spacetime, Sogang University, Seoul 04107, Korea

Abstract

It is shown that anisotropic matter black holes with two parameters w and K are identified as nonlinear electrodynamics (NED) black holes with power-index s and charge term $\xi(s, q)$ by introducing a NED term. These NED black holes include constant scalar hair ($s = 1$), charged quantum Oppenheimer-Snyder ($s = 3/2$), and Einstein-Euler-Heisenberg ($s = 2$) black holes derived from their known actions. Rotating NED black holes can be obtained from rotating anisotropic matter black holes when replacing w and K by $2s - 1$ and $\xi(s, q)$. The extremal rotating NED black holes being the boundary between rotating charged NED black hole and naked singularity are derived as functions of the rotation parameter $a(q)$.

¹*email: ysmyoung@inje.ac.kr*

²*email: warrior@sogang.ac.kr*

1 Introduction

Recent observational reports regarding cosmic expansion and galactic supermassive black holes would appear to challenge the existing paradigm of our Universe [1, 2, 3, 4, 5, 6], thus prompting a reassessment of our fundamental cosmological models. The current cosmological model suggests that dark energy and dark matter constitute most of the total energy budget, while ordinary matter only accounts for about a few percents [7]. This realization of our limited knowledge underscores the necessity for a more cautious and humble approach to exploring the Universe.

The majority of compact objects would be rotating in the Universe, and there has been a concomitant increase in interest in solutions to Einstein's equations for rotating black holes [8, 9]. Furthermore, supermassive black holes have been found at the centers of galaxies [10, 11]. These black holes coexist with dark matter in astrophysical environments and are becoming a focal point of study [12]. Accordingly, research interests are increasingly shifting towards black hole solutions that incorporate matter fields, moving beyond Einstein's vacuum solutions [13, 14, 15, 16, 17].

Anisotropic matter black holes (AMBHs) with equation of state (anisotropic) parameter w and energy density K were derived from an anisotropic fluid with equation of states ($p_1 = -\rho, p_2 = w\rho$) [18]. Here, w and K may be regarded as hairs of AMBH. It is worth to note that AMBHs and their charged solution were also found from the quintessential energy-momentum tensor $T_{\mu\nu}^q$ [19, 20]. We note that the power-law hairy black hole solution was found from the Einstein-Kalb-Ramond theory [21]. Furthermore, rotating charged AMBH solution were derived by making use of the Newman-Janis algorithm [22]. This solution is considered as an extension of the Kerr-Newman (KN) black hole. Its shadow analysis was performed by discussing the effect of the anisotropic term (K/r^{2w-2}) [23]. On the other hand, the anisotropic (exotic) fluid could be used to construct the Morris-Thorne-type wormhole under the condition of $p_1 + 2p_2 = -\rho$ [24].

So far, there is no known action corresponding to this anisotropic fluid and thus it may restrict researchers from a further study on AMBHs.

In the present work, we introduce the nonlinear electrodynamics (NED) term of \mathcal{F}^s with \mathcal{F} the Maxwell term [25] as the corresponding action with a magnetically charged configuration. We identify AMBH with two parameters w and K exactly as NED black holes with power index s and charge term $\xi(s, q)$. These NED black holes include interesting known black holes: Schwarzschild-de Sitter ($s = 0, w = -1$), constant scalar hair ($s = w = 1$), charged quantum Oppenheimer-Snyder ($s = 3/2, w = 2$), Einstein-Euler-Heisenberg ($s = 2, w = 3$), and Ned black holes ($s = 3, w = 5$). Rotating charged AMBHs can describe rotating charged NED black holes when replacing anisotropic parameter w and density K by power index s and charge term $\xi(s, q)$.

The paper is organized as follows. In Sect. 2, we briefly mention how to find AMBHs from an anisotropic fluid with barotropic equation of state but not an anisotropic matter action. In

Sec. 3, we obtain NED black holes including known black hole solutions by considering a power-law of Maxwell term as an anisotropic matter action. Sec. 4 is devoted to discussing rotating charged NED black holes and their extremal rotating NED black holes which are the boundary between rotating charged NED black holes and naked singularity. Finally, we summarize our results and discuss on relevant issues in Sec. 5.

2 AMBHs

We wish to mention briefly how to obtain AMBHs. First of all, we consider the anisotropic energy-momentum tensor

$$T_{\mu}^{\text{AM},\nu} = \text{diag}[-\rho, p_1, p_2, p_3] = \rho \cdot \text{diag}[-1, w_1, w_2, w_3], \quad (1)$$

whose barotropic equation of state is described by

$$p_i = w_i \rho. \quad (2)$$

For the anisotropic fluid with $p_1 = -\rho$ ($w_1 = -1$) in the radial direction and $p_2 = p_3 = w\rho$ ($w_2 = w_3 = w$) in the angular direction, solving $p_2 = -\rho - r\rho'/2$ with $f(r) = 1 - 2m(r)/r$ leads to the energy density, the mass function, and the metric function

$$\rho = \frac{(1-2w)K}{8\pi r^{2w+2}}, \quad m(r) = M + \frac{K}{2r^{2w-1}}, \quad f(r) = 1 - \frac{2M}{r} - \frac{K}{r^{2w}}. \quad (3)$$

One may introduce r_o as a length dimension defined by $r_o^{2w} = (1-2w)K$. If one is interested in asymptotically flat geometries, it is worthwhile to analyze the case of $w > 1/2$. Then, K is negative for $w > 1/2$ when the energy density is positive. This case will correspond to $s > \frac{3}{4}$ for $\xi(s, q) < 0$.

Then, we consider the Einstein-Maxwell theory with unknown anisotropic matter term \mathcal{L}_{AM} [22, 26]

$$I_{\text{CAM}} = \int d^4x \sqrt{-g} \left[\frac{1}{16\pi} (R - F_{\mu\nu} F^{\mu\nu}) + \mathcal{L}_{\text{AM}} \right], \quad (4)$$

where $-2\frac{\partial \mathcal{L}_{\text{AM}}}{\partial g^{\mu\nu}} + \mathcal{L}_{\text{AM}}$ is assumed to arrive at Eq.(1).

Its charged black hole solution is given by

$$ds_{\text{CAM}}^2 = -f(r)dt^2 + \frac{dr^2}{f(r)} + r^2(d\theta^2 + \sin^2\theta d\phi^2), \quad (5)$$

where

$$\tilde{f}(r) = 1 - \frac{2M}{r} + \frac{q^2}{r^2} - \frac{K}{r^{2w}}. \quad (6)$$

Here, ADM mass M , charge q , and two parameters w and K may be regarded as hairs for the charged AMBH. In this case, one does not know their origin of w and K because the energy-momentum $T_{\mu\nu}^{\text{AM}}$ was used to derive the solution.

3 NED black holes

First of all, we remind the reader that the AMBH solutions (3) and (6) were derived from the anisotropic fluid of $w_1 = -1$ with various values of $w_2 = w$ as an extension of Reissner-Nordström (RN) black hole whose energy-momentum tensor is given by $T_{\mu}^{\text{RN } \nu} = \frac{2q^2}{r^4} \text{diag}[-1, -1, 1, 1]$. This indicates a hint for choosing \mathcal{L}_{AM} as an extension of the Maxwell term $\mathcal{F} = F_{\mu\nu} F^{\mu\nu}$.

Hence, let us introduce the Einstein-NED action proposed by Hassaine and Martinez [25]

$$I_{\text{HM}} = \int d^4x \sqrt{-g} \left[\frac{R}{16\pi} - \xi \mathcal{F}^s \right] \quad (7)$$

with an action parameter ξ for the NED term of \mathcal{F} to the power of s . In this case, the Einstein equation takes the form

$$G_{\mu}^{\nu} = 8\pi T_{\mu}^{\nu}, \quad (8)$$

whose energy-momentum tensor is given by

$$T_{\mu}^{\nu} = -\xi \left(\mathcal{F}^s \delta_{\mu}^{\nu} - 4s \mathcal{F}^{s-1} F_{\mu\rho} F^{\nu\rho} \right). \quad (9)$$

Its non-linear Maxwell equation is given by

$$\nabla_{\mu} \left(\mathcal{F}^{s-1} F^{\mu\nu} \right) = 0. \quad (10)$$

For a magnetically charged case, one finds

$$A_{\phi} = -q \cos \theta \rightarrow F_{\theta\phi} = q \sin \theta \rightarrow \mathcal{F} = \frac{2q^2}{r^4} (= 2B^2) \quad (11)$$

with a magnetic field $B = |\mathbf{B}|$. In this case, its energy-momentum tensor takes the form [28]

$$T_{\mu}^{\nu} = \frac{2^s \xi q^{2s}}{r^{4s}} \text{diag}[-1, -1, 2s-1, 2s-1], \quad (12)$$

which satisfies all (null, weak, strong) energy conditions for $\xi > 0$ and $s \geq \frac{1}{2}$ except the dominant energy condition of $\rho \geq |p_i|$. The mass function is derived as

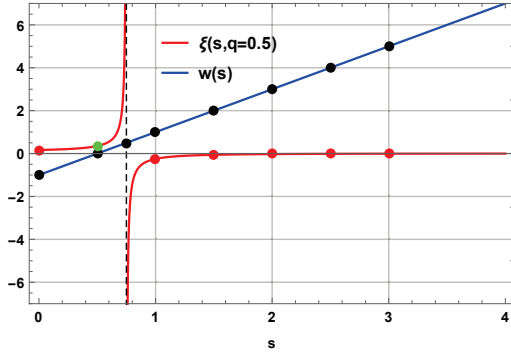
$$m(r) = 4\pi \int^r r'^2 \rho(r') dr' = M + \frac{2^{s+2} \pi \xi q^{2s}}{(3-4s)r^{4s-3}}. \quad (13)$$

Then, we obtain the metric function to describe the NED black hole solution

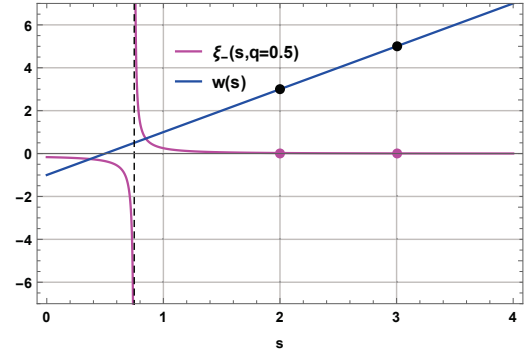
$$h(r) = 1 - \frac{2M}{r} - \frac{\xi(s, q)}{r^{4s-2}}, \quad \xi(s, q) = \pi \xi \frac{2^{s+3} q^{2s}}{3-4s}. \quad (14)$$

Importantly, comparing Eq.(3) with Eq.(14) leads to

$$w = 2s - 1, \quad K = \xi(s, q). \quad (15)$$



(a) $\xi = \frac{1}{16\pi}$ and $q = 0.5$



(b) $\xi = -\frac{1}{16\pi}$ and $q = 0.5$

Figure 1: (a) Charge term $\xi(s, q = 0.5)$ is as a function of s . For $0 < s < \frac{3}{4}$, $\xi(s, 0.5)$ increases, it blows up at $s = \frac{3}{4}$ (dashed line), and it increases negatively for $s > \frac{3}{4}$. Equation of state parameter $w(s)$ is as a function of s . It is negative for $0 < s < \frac{1}{2}$, it is zero at $s = \frac{1}{2}$, and it is positive for $s > \frac{1}{2}$. Eight black dots are displaced for Table 1. Six red dots including one green dot (not black hole) are shown for Fig. 3(a). (b) $\xi_-(s, q = 0.5)$ is as a function of s . Two magenta dots represent EEH and Ned black holes.

Here, if one chooses the action parameter $\xi = \frac{1}{16\pi}$, there is no ambiguity to describe $\xi(s, q)$ in terms of charge q and power-index s . Figure 1 shows the plot of the charge terms, $\xi(s, q = 0.5)$ and $\xi_-(s, q = 0.5)$, as functions of s . For $0 < s < \frac{3}{4}$, $\xi(s, 0.5)$ increases, it blows up at $s = \frac{3}{4}$, and it increases negatively. Also, the equation of state parameter $w(s)$ is a linear function of s : negative for $0 < s < \frac{1}{2}$; zero at $s = \frac{1}{2}$; positive for $s > \frac{1}{2}$. For $s = \frac{1}{2}$ (its action: $\sqrt{\mathcal{F}}$), its anisotropic term $\xi(s, q)/r^{4s-2}$ becomes constant, while this term blows up at $s = \frac{3}{4}$ (its action: $\mathcal{F}^{3/4}$). Hence, the latter is not a proper case. This approach recovers famous known black hole solutions (see Table 1). For $s = 0$ ($w = -1$), Eq.(14) represents Schwarzschild-de Sitter (SdS) black hole [27]. The $s = 1$ ($w = 1$) case indicates the RN black hole. In case of $s = 3/2$ ($w = 2$), Eq.(14) indicates the charged quantum Oppenheimer-Snyder (cqOS) black hole [28] which may become quantum Oppenheimer-Snyder (qOS) black hole for selecting $P = M$ [29]. Now, we would like to mention that the electrically charged black hole solution was derived from the same action (7) [28]. Even though its form differs slightly from Eq.(14), it can describe the same thing. In this sense, the power-index s is not considered as a hair of NED black holes but a sorter of NED black holes. The charge q in $\xi(s, q)$ can be regarded as a hair for NED black holes with the mass M .

It is worth noting that its horizon structure obtained from $h(r) = 0$ depends crucially on the power-index s . So, one could not find its horizon structure for general s . As was shown in Fig. 2, there exist two horizons: (a) $s = 0$, r_{\pm} represents the outer/Cauchy horizons for SdS black hole for $0 < M < 0.471$. (b) $s = 1, 3/2$ and $M = 1$. r_{\pm} represents the outer/inner horizons of RN and cqOS black holes existing for $0 < q < 1$ and $0 < q < 1.53$. The allowed region q for cqOS is larger than RN. For a given s -black hole solution, the corresponding outer

s	0	1/2	3/4	1	3/2	2	$\frac{5}{2}$	3
$w(s)$	-1	0	1/2	1	2	3	4	5
$K/\xi(s, q)$	$\frac{1}{6}$	$\frac{q}{\sqrt{2}}$	∞	$-q^2 / -q_s^2$	$-\frac{\sqrt{2}q^3}{3}$	$-\frac{2q^4}{5}$	$-\frac{2\sqrt{2}q^5}{7}$	$-\frac{4q^6}{9}$
BH	SdS[27]	N.A.	N.A.	RN/CSH	cqOS	EEH[32]		Ned
RBH	KdS	RG	N.A.	KN[9]		REEH[34]		

Table 1: Table for classification of known black holes with respect to s and $w(s)$ for $\xi = \frac{1}{16\pi}$. (R)BH, SdS, RN, CSH[30, 31], cqOS[28], (R)EEH, Ned[35], KdS[36], and RG[38] denote (rotating) black hole, Schwarzschild-de Sitter, Reissner-Nordström, constant scalar hair, charged quantum Oppenheimer-Snyder, (Rotating) Einstein-Euler-Heisenberg, nonlinear electrodynamics, Kerr-de Sitter, and rotating galaxy. Note that $\xi = -\frac{1}{16\pi}$ is chosen for (R)EEH and Ned black holes.

horizon defined by r_+ can be used to compute all thermodynamic quantities, scalarization, shadow radius analysis, and greybody and quasinormal modes computations.

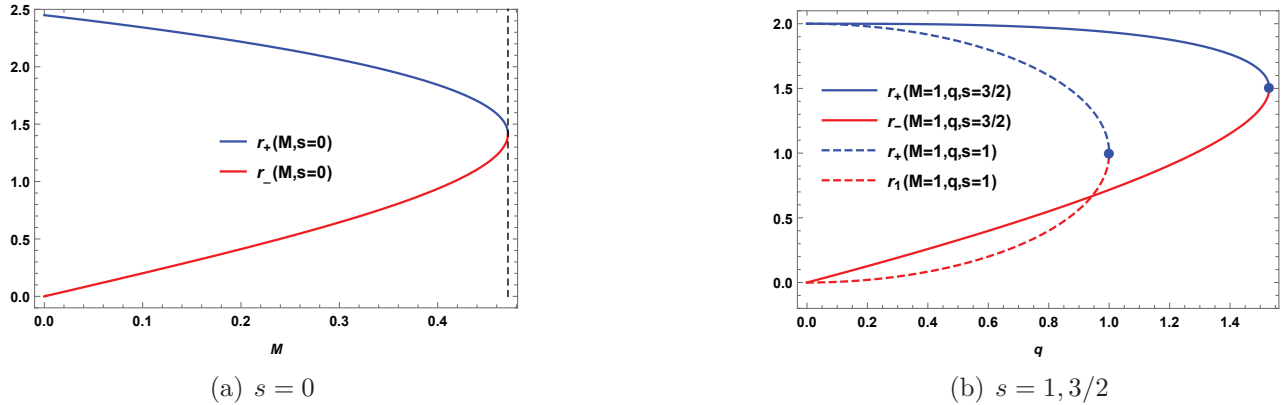


Figure 2: Horizon structure. (a) For $s = 0$ and $\xi = \frac{1}{16\pi}$, r_{\pm} represents the outer/Cauchy horizons of Schwarzschild-de Sitter black hole for $0 < M < 0.471$. The dashed line is located at extremal point $M_e = 0.471$. (b) For $s = 1, 3/2$, $\xi = \frac{1}{16\pi}$ and $M = 1$. r_{\pm} represents the outer/inner horizons of RN and cqOS black holes for $0 < q < 1$ and $0 < q < 1.53$. Two blue dots are located at extremal points (1,1) and (1.53,1.5) and they will also be displaced in Fig. 3(a).

Considering the Einstein-Maxwell theory with the NED term

$$I_{\text{EMN}} = \int d^4x \sqrt{-g} \left[\frac{1}{16\pi} (R - F_{\mu\nu} F^{\mu\nu}) - \xi \mathcal{F}^s \right], \quad (16)$$

the charged NED black hole solution is given by

$$\tilde{h}(r) = 1 - \frac{2M}{r} + \frac{q^2}{r^2} - \frac{\xi(s, q)}{r^{4s-2}}. \quad (17)$$

In this case, the mass M and charge q are regarded as hairs, while s is a sorter for charged NED black holes. We have its two known black hole solutions. For $s = 1 (w = 1)$, Eq.(17) represents constant scalar hair (CSH) black hole derived from the Einstein-Maxwell-conformally coupled scalar theory [30, 31]. In case of $s = 2 (w = 3)$, Eq.(17) indicates the Einstein-Euler-Heisenberg (EEH) black hole [32] which includes the QED effect of vacuum polarization [33]. The $s = 3 (w = 5)$ case leads to Ned black hole. As is shown in Table 1, there are known black hole solution derived from the Einstein-NED action.

4 Rotating charged NED black holes

The rotating charged black hole solution with NED matter is obtained by applying the Newman-Janis algorithm to a static spherically symmetric solution Eq.(17) as [39, 40, 22]

$$\begin{aligned} ds^2 &= -F(r, \theta)dt^2 - 2[1 - F(r, \theta)]a \sin^2 \theta dt d\phi + \frac{\Sigma}{\rho^2} \sin^2 \theta d\phi^2 + \frac{\rho^2}{\Delta} dr^2 + \rho^2 d\theta^2 \\ &= -\frac{\Delta}{\rho^2} (dt - a \sin^2 \theta d\phi)^2 + \frac{\sin^2 \theta}{\rho^2} [adt - (r^2 + a^2)d\phi]^2 + \frac{\rho^2}{\Delta} dr^2 + \rho^2 d\theta^2, \end{aligned} \quad (18)$$

where

$$\begin{aligned} F(r, \theta) &= 1 - \frac{2Mr - q^2 + \xi(s, q)r^{4(1-s)}}{\rho^2}, \quad a = \frac{J}{M}, \quad \rho^2 = r^2 + a^2 \cos^2 \theta, \\ \Delta &= r^2 + a^2 + q^2 - 2Mr - \xi(s, q)r^{4(1-s)}, \\ \Sigma &= \rho^2(r^2 + a^2) + [2Mr - q^2 + \xi(s, q)r^{4(1-s)}]a^2 \sin^2 \theta. \end{aligned} \quad (19)$$

The $\xi(s, q) = 0$ case leads to the KN black hole and $\xi(s, q) = 0$ with $q = 0$ corresponds to the Kerr black hole [8], regarding as two references for rotating black hole. At this stage, we mention that the event (outer) horizon (r_+) for the spacetime (18) is located at the largest radius as a solution to $\Delta = 0$ [41], leading to the event horizon for KN black hole with $\xi(s, q) = 0$. The region between the event horizon and the infinite-redshift surface of $F(r, \theta) = 0$ is called the ergosphere [42]. In this case, its horizon structure depends on $s > 0$ and ξ critically, so we encounter a difficulty to display it. However, requiring $\Delta = 0$ and $\Delta' = 0$ simultaneously, the extremal rotating black hole whose horizons are degenerate is determined by [43]

$$2s - 1 = \frac{a^2 + q^2 - Mr}{\Delta_{\text{KN}}}, \quad \xi(s, q) = \frac{\Delta_{\text{KN}}}{r \frac{2r(r-M)}{\Delta_{\text{KN}}}} \quad (20)$$

with $\Delta_{\text{KN}} = r^2 - 2Mr + a^2 + q^2$. This extremal rotating black hole represents a boundary between rotating charged NED black hole and naked singularity.

As an example, we consider the extremal NED black holes. Figure 3 shows curves for extremal NED black hole, in which w is given by $2s - 1$. Solid curve in Fig. 3(a) includes

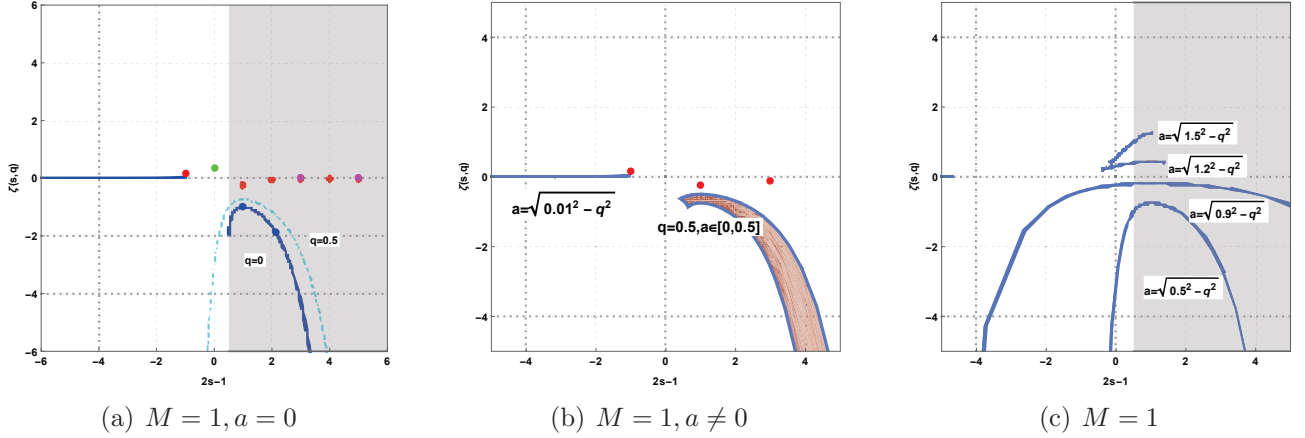


Figure 3: (a) Curves for extremal NED black holes with $q = 0, q = 0.5$ and $a = 0$. All six red dots with two magenta dots shown in Figs. 1(a) and 1(b) are located above these extremal curves. The shaded region of asymptotically flat black holes denotes the region of $s > \frac{3}{4}$ ($w > 1/2$). (b) Curves for extremal rotating NED black holes with $q = 0, 0.5$ and $a \neq 0$. (c) Four curves of extremal rotating NED black holes : $a(q) = \sqrt{0.5^2 - q^2}$, $\sqrt{0.9^2 - q^2}$, $\sqrt{1.2^2 - q^2}$, and $\sqrt{1.5^2 - q^2}$. The shaded region indicates for $s > \frac{3}{4}$. Each solid curve separating the black hole (above curve) from naked singularity (below curve) are parametrically described by Eq.(20).

two blue dots for extremal RN BH at $(1, -1)$ and extremal cqOS BH at $(2.13, -1.88)$ shown in Fig. 2(b). This is given by $2s - 1 = -Mr/\Delta_S$ and $\xi(s, q) = \Delta_S/r^{2r(r-M)/\Delta_S}$ with $\Delta_S = r^2 - 2Mr$. The extremal charged NED black holes with $q = 0.5$ (dashed curve in Fig. 3(a)) are determined by $2s - 1 = (q^2 - Mr)/\Delta_{RN}$ and $\xi(s, q) = \Delta_{RN}/r^{2r(r-M)/\Delta_{RN}}$ with $\Delta_{RN} = r^2 - 2Mr + q^2$. Their extremal black hole curves are shown in Fig. 3(a). All six red dots with one green dot shown in Fig. 1(a) are also located above the extremal curves in Fig. 3(a). The first red dot denotes SdS, while the green dot represents an object but not black hole because there is no corresponding extremal curve. All five dots located inside the shaded region represent as asymptotically flat NED black holes shown in Fig. 1(a). At this stage, we wish to point out that two dots at $w(= 2s - 1) = 3, 5$ include two red dots of $\xi(s, q) = -0.025, -0.0069$ (Fig. 1(a)) for NED black holes and two magenta dots of $\xi(s, q) = 0.025, 0.0069$ (Fig. 1(b)) for charged NED black holes (EEH and Ned). This implies that $s(w)$ in x -axis classifies NED black holes, while $\xi(s, q)(K)$ in y -axis denotes the corresponding charge term.

For extremal rotating black holes with $M = 1, q = 0, 0.5$, see Fig. 3(b) which includes three red dots for KdS, KN, and REEH black holes. These all are located above extremal curves. On the other hand, plotting the curves parametrically when choosing $a(q)$ leads to four curves where extremal rotating NED black holes exist, as is shown in Fig. 3(c). Unlike the extremal KN spacetime with $q^2 + a^2 \leq M^2 (= 1)$ (below two negative curves), extremal rotating NED black holes can allowed for $q^2 + a^2 > M^2 (= 1)$ (above two positive curves). Also, the existence s -region for the former is larger than that for the latter. We note that each solid curve separates

rotating charged NED black hole (above curve) from naked singularity (below curve).

In addition, we may read off the orthonormal frame from Carter's form of Eq. (18). The corresponding covariant tetrad is given by

$$\begin{aligned} e_{\hat{\mu}}^{\hat{t}} &= \frac{\sqrt{\Delta}}{\rho}(1, 0, 0, -a \sin^2 \theta), & e_{\hat{\mu}}^{\hat{\phi}} &= \frac{\sin \theta}{\rho}(a, 0, 0, -(r^2 + a^2)), \\ e_{\hat{\mu}}^{\hat{r}} &= \frac{\rho}{\sqrt{\Delta}}(0, 1, 0, 0), & e_{\hat{\mu}}^{\hat{\theta}} &= \rho(0, 0, 1, 0) \end{aligned} \quad (21)$$

and the contravariant tetrad takes the form [40, 44]

$$\begin{aligned} e_{\hat{t}}^{\mu} &= \frac{1}{\rho\sqrt{\Delta}}(r^2 + a^2, 0, 0, a), & e_{\hat{\phi}}^{\mu} &= -\frac{1}{\rho \sin \theta}(a \sin^2 \theta, 0, 0, 1), \\ e_{\hat{r}}^{\mu} &= \frac{\sqrt{\Delta}}{\rho}(0, 1, 0, 0), & e_{\hat{\theta}}^{\mu} &= \frac{1}{\rho}(0, 0, 1, 0). \end{aligned} \quad (22)$$

Making use of Eq.(22), an observer located at this orthonormal frame can read physical quantities of energy density and pressures as

$$\varepsilon(= -p_{\hat{r}}) = \frac{G_{\mu\nu} e_{\hat{t}}^{\mu} e_{\hat{t}}^{\nu}}{8\pi} = \varepsilon_e + \varepsilon_{\text{AM}} = \frac{1}{8\pi\rho^4} \left[q^2 + 2^{s+3} \pi \xi q^{2s} r^{4(1-s)} \right], \quad (23)$$

$$p_{\hat{\theta}}(= p_{\hat{\phi}}) = \frac{G_{\mu\nu} e_{\hat{\theta}}^{\mu} e_{\hat{\theta}}^{\nu}}{8\pi} = \frac{[(s+1)q^2\rho^2 + 2^{s+2}\pi\xi q^{2s}r^{4(1-s)}][(2s-1)\rho^2 - a^2 \cos^2 \theta]}{4\pi r^2 \rho^4}. \quad (24)$$

In the non-rotating limit of $a \rightarrow 0$, one obtains the static energy density and pressure from Eqs.(23) and (24)

$$\varepsilon_s = \frac{q^2}{8\pi r^4} + \frac{2^s \xi q^{2s}}{r^{4s}}, \quad p_{\hat{\theta}}^s = \frac{(s+1)q^2}{4\pi r^4} + \frac{(2s-1)2^s \xi q^{2s}}{r^{4s}}. \quad (25)$$

It is important to note that the parameters $\xi(s, q)$ and s control the charge term and anisotropy of the NED matter.

As shown in Table 1 (Fig. 1(b)), there exist three rotating NED black holes for $s = 0, 1, 2$ ($w = -1, 1, 3$). Hence, one expects to read off a lot of rotating charged NED black holes from Fig. 3(c). Finally, we mention that for $s = 1/2$ ($w = 0$) [37], its action described the flat rotation curve of a galaxy [38].

5 Conclusion

Although research on anisotropic fluid black holes is ongoing, it has been difficult to construct black hole solutions starting from an action. This is primarily due to the absence of a recognized action for such a fluid matter. In this study, we have introduced a nonlinear electrodynamics (NED) term to construct black hole solutions starting from the corresponding explicit action.

We have identified anisotropic matter black holes (AMBHs) with anisotropic parameter w and energy density K as nonlinear electrodynamics (NED) black holes with power-index s and $\xi(s, q)$. This implies that AMBHs have nothing but NED black holes. Here, s is identified with a classifier of NED black holes, while $\xi(s, q)$ corresponds to the charge term including charge q as a hair. These NED black holes have included Schwarzschild-de Sitter with $q = 0$ ($w = -1$), Reissner-Nordström and constant scalar hair ($w = 1$), charged quantum Oppenheimer-Snyder ($w = 2$), Einstein-Euler-Heisenberg ($w = 3$), and Ned ($w = 5$) black holes derived from their known actions.

Finally, we would like to mention that rotating charged AMBHs can describe rotating charged NED black holes as well when replacing w and K by s and $\xi(s, q)$. The extremal rotating NED curves being the boundary between rotating charged NED black hole and naked singularity were derived as functions of the rotation parameter $a(q)$.

Acknowledgments

Y. S. M (RS-2022-NR069013), W. L (RS-2022-NR075087), and Center for Quantum Space-time (CQUeST) of Sogang University (RS-2020-NR049598) were supported by Basic Science Research Program through the National Research Foundation of Korea funded by the Ministry of Education. We are grateful to Hyeong-Chan Kim for his hospitality during our visit to the Tangeumdae Workshop.

References

- [1] M. Abdul Karim *et al.* [DESI], Phys. Rev. D **112**, no.8, 083515 (2025) [arXiv:2503.14738 [astro-ph.CO]].
- [2] J. Son, Y. W. Lee, C. Chung, S. Park and H. Cho, Mon. Not. Roy. Astron. Soc. **544**, no.1, 975-987 (2025) [arXiv:2510.13121 [astro-ph.CO]].
- [3] S. Capozziello, H. Chaudhary, T. Harko and G. Mustafa, Phys. Dark Univ. **51**, 102196 (2026) [arXiv:2512.10585 [astro-ph.CO]].
- [4] K. Akiyama *et al.* [Event Horizon Telescope], Astron. Astrophys. **704**, A91 (2025) [arXiv:2509.24593 [astro-ph.HE]].
- [5] R. Dahale *et al.* [Event Horizon Telescope], Astron. Astrophys. **699**, A279 (2025) [arXiv:2505.10333 [astro-ph.HE]].
- [6] K. Akiyama *et al.* [Event Horizon Telescope], Astron. Astrophys. **693**, A265 (2025).
- [7] N. Aghanim *et al.* [Planck], Astron. Astrophys. **641**, A1 (2020) [arXiv:1807.06205 [astro-ph.CO]].

- [8] R. P. Kerr, Phys. Rev. Lett. **11**, 237-238 (1963).
- [9] E. T. Newman, E. Couch, K. Chinnapared, A. Exton, A. Prakash and R. Torrence, J. Math. Phys. **6**, 918-919 (1965).
- [10] A. M. Ghez, S. Salim, N. N. Weinberg, J. R. Lu, T. Do, J. K. Dunn, K. Matthews, M. Morris, S. Yelda and E. E. Becklin, *et al.* Astrophys. J. **689**, 1044-1062 (2008) [arXiv:0808.2870 [astro-ph]].
- [11] S. Gillessen, F. Eisenhauer, S. Trippe, T. Alexander, R. Genzel, F. Martins and T. Ott, Astrophys. J. **692**, 1075-1109 (2009) [arXiv:0810.4674 [astro-ph]].
- [12] P. G. S. Fernandes and V. Cardoso, Phys. Rev. Lett. **135**, no.21, 211403 (2025) [arXiv:2507.04389 [gr-qc]].
- [13] S. Datta and C. Singha, [arXiv:2602.10579 [gr-qc]].
- [14] R. A. Konoplya and A. Zhidenko, Phys. Rev. D **113**, no.4, 043011 (2026) [arXiv:2511.03066 [gr-qc]].
- [15] J. Podolsky and H. Ovcharenko, Phys. Rev. Lett. **135**, no.18, 181401 (2025) [arXiv:2507.05199 [gr-qc]].
- [16] H. Ovcharenko, J. Podolsky and M. Astorino, Phys. Rev. D **111**, no.8, 084016 (2025) [arXiv:2501.07537 [gr-qc]].
- [17] H. C. Kim and W. Lee, Eur. Phys. J. C **85**, no.11, 1245 (2025) [arXiv:2503.06961 [gr-qc]].
- [18] I. Cho and H. C. Kim, Chin. Phys. C **43**, no.2, 025101 (2019) [arXiv:1703.01103 [gr-qc]].
- [19] V. V. Kiselev, Class. Quant. Grav. **20**, 1187-1198 (2003) [arXiv:gr-qc/0210040 [gr-qc]].
- [20] B. Toshmatov, Z. Stuchlík and B. Ahmedov, Eur. Phys. J. Plus **132**, no.2, 98 (2017) [arXiv:1512.01498 [gr-qc]].
- [21] R. Kumar, S. G. Ghosh and A. Wang, Phys. Rev. D **101**, no.10, 104001 (2020) [arXiv:2001.00460 [gr-qc]].
- [22] H. C. Kim, B. H. Lee, W. Lee and Y. Lee, Phys. Rev. D **101**, no.6, 064067 (2020) [arXiv:1912.09709 [gr-qc]].
- [23] B. H. Lee, W. Lee and Y. S. Myung, Phys. Rev. D **103**, no.6, 064026 (2021) [arXiv:2101.04862 [gr-qc]].
- [24] M. S. Morris and K. S. Thorne, Am. J. Phys. **56**, 395-412 (1988).
- [25] M. Hassaine and C. Martinez, Class. Quant. Grav. **25**, 195023 (2008) [arXiv:0803.2946 [hep-th]].

- [26] S. J. C., K. R., K. Hegde, K. M. Ajith, S. Punacha and A. N. Kumara, Phys. Rev. D **111**, no.6, 064034 (2025) [arXiv:2411.11629 [gr-qc]].
- [27] P. R. Brady, C. M. Chambers, W. Krivan and P. Laguna, Phys. Rev. D **55**, 7538-7545 (1997) [arXiv:gr-qc/9611056 [gr-qc]].
- [28] S. H. Mazharimousavi, Eur. Phys. J. C **85**, no.6, 667 (2025) [arXiv:2502.10457 [gr-qc]].
- [29] J. Lewandowski, Y. Ma, J. Yang and C. Zhang, Phys. Rev. Lett. **130**, no.10, 101501 (2023) [arXiv:2210.02253 [gr-qc]].
- [30] M. Astorino, Phys. Rev. D **88**, no.10, 104027 (2013) [arXiv:1307.4021 [gr-qc]].
- [31] Y. S. Myung, Gen. Rel. Grav. **56**, no.5, 60 (2024) [arXiv:2401.08200 [gr-qc]].
- [32] H. Yajima and T. Tamaki, Phys. Rev. D **63**, 064007 (2001) [arXiv:gr-qc/0005016 [gr-qc]].
- [33] W. Heisenberg and H. Euler, Z. Phys. **98**, no.11-12, 714-732 (1936) [arXiv:physics/0605038 [physics]].
- [34] N. Bretón, C. Lämmerzahl and A. Macías, Class. Quant. Grav. **36**, no.23, 235022 (2019).
- [35] Y. S. Myung, [arXiv:2505.00280 [gr-qc]].
- [36] S. Akcay and R. A. Matzner, Class. Quant. Grav. **28**, 085012 (2011) [arXiv:1011.0479 [gr-qc]].
- [37] M. Barriola and A. Vilenkin, Phys. Rev. Lett. **63**, 341 (1989).
- [38] V. C. Rubin and W. K. Ford, Jr., Astrophys. J. **159**, 379-403 (1970).
- [39] R. H. Boyer and R. W. Lindquist, J. Math. Phys. **8**, 265 (1967).
- [40] B. Carter, Commun. Math. Phys. **10**, no.4, 280-310 (1968).
- [41] B. Carter, J. Math. Phys. **10**, 70-81 (1969).
- [42] R. Ruffini and J. A. Wheeler, *RELATIVISTIC COSMOLOGY AND SPACE PLATFORMS*, PRINT-70-2077.
- [43] J. Badía and E. F. Eiroa, Phys. Rev. D **102**, no.2, 024066 (2020) [arXiv:2005.03690 [gr-qc]].
- [44] M. Azreg-Ainou, Phys. Lett. B **730**, 95-98 (2014) [arXiv:1401.0787 [gr-qc]].